

# A Learning Approach to Understand How Spinal Cord Learns Multiple Behaviors

Yuyao Shi

CMU-RI-TR-23-61

August 06, 2023



The Robotics Institute  
School of Computer Science  
Carnegie Mellon University  
Pittsburgh, PA

**Thesis Committee:**

Hartmut Geyer, *chair*

Nancy Pollard

Omar Refy

*Submitted in partial fulfillment of the requirements  
for the degree of Master of Science in Robotics.*

Copyright © 2023 Yuyao Shi. All rights reserved.



## Abstract

The spinal cord plays a crucial role in the control of human locomotion, generating motor patterns and coordinating reflex responses to sensory signals. Although this spinal control is traditionally viewed as a simple relay system, more recent neurophysiological evidence points to a remarkable functional plasticity of the spinal circuitry, indicating that it can, to some extent, learn the control of locomotion. In line with this observation, a recent computational model of human hopping demonstrated how spinal control learning may be achieved by a transfer of control from the brain to the spinal cord through heterosynaptic modulation of spinal interneurons. However, this model did not account for the multiple behaviors that the spinal cord commonly has to accommodate and lacked an explicit mechanism by which the human nervous system could decide when to engage or disengage this control transfer between the brain and cord. To overcome these drawbacks, we here extend this model by incorporating physiologically plausible spinal controller and responsibility circuit networks that enable the automatic selection and learning of multiple behaviors. Equipped with these adaptive networks, we demonstrate that the spinal control of the model can simultaneously learn competing behaviors such as the generation of human hopping motions and the recovery from infrequent and random push disturbances while automatically deciding when to rely on spinal control or re-engage control supervision by the brain. In addition, we find that the learned spinal networks contain muscle reflexes well-known from physiological experiments. Thus, our results not only suggest specific neural mechanisms for the spinal plasticity observed in neurophysiological experiments but also may help to elucidate how multiple behaviors are controlled at the spinal cord level.



## Acknowledgments

I would like to take this opportunity to express my deepest gratitude to all those who have supported and guided me throughout the completion of this thesis.

First and foremost, I am immensely grateful to my thesis advisor, Prof. Hartmut Geyer, for his invaluable guidance, unwavering support, and insightful feedback. His expertise and encouragement have been instrumental in shaping this research and enhancing my academic abilities.

I am also thankful to the faculty members of Prof. Nancy Pollard and Omar Refy, who have provided valuable insight to my thesis.

I extend my heartfelt appreciation to my family for their unconditional love and support. Their belief in me and their encouragement during challenging times have been a driving force behind the completion of this thesis.

I would like to acknowledge the assistance and cooperation of my labmates, Ashwin, Bill, and Russell, who provided valuable insights and constructive criticism that helped refine my work.

Last but not least, I am grateful to all the authors, researchers, and scholars whose work served as the foundation for my study. Their contributions to the field have been instrumental in shaping the ideas presented in this thesis.

This thesis would not have been possible without the collective support and encouragement of all these individuals, and for that, I am eternally grateful.



# Contents

<b>1</b>	<b>Introduction</b>	<b>1</b>
<b>2</b>	<b>Methods</b>	<b>5</b>
2.1	Musculo-Skeletal Mechanics . . . . .	5
2.2	Brain Reference Controller . . . . .	6
2.3	The spinal cord controller network . . . . .	10
2.3.1	Spinal cord learning . . . . .	11
2.3.2	Switch mechanism between brain and spinal cord . . . . .	14
<b>3</b>	<b>Results</b>	<b>15</b>
3.1	Does the proposed framework learn? . . . . .	15
3.2	Functional roles of each controller . . . . .	16
3.2.1	Stance phase . . . . .	18
3.2.2	Swing phase . . . . .	19
3.3	Reason for switching back to the brain control . . . . .	21
<b>4</b>	<b>Discussion</b>	<b>23</b>
4.1	Future work . . . . .	24
<b>5</b>	<b>Conclusions</b>	<b>25</b>
<b>A</b>	<b>Modeling parameters</b>	<b>27</b>
	<b>Bibliography</b>	<b>29</b>

# List of Figures

2.1	Kinematics of the model and muscles involved. . . . .	7
2.2	Schematic of the brain controller . . . . .	9
2.3	Spinal cord controller structure . . . . .	11
2.4	Learning framework . . . . .	13
3.1	Spinal cord proportion over training. . . . .	16
3.2	Weights at the spinal cord converge to similar controllers. (a)Activation patterns of controllers over the stance and swing cycle. (b)PCA analysis of all weights from five trials.(c)Cumulative percentage of the active pathways . . . . .	17
3.3	Average stimulation contribution in stance phase . . . . .	19
3.4	Average kinematics of the body. . . . .	20
3.5	Average stimulation contribution in swing phase . . . . .	20
3.6	Average kinematic trajectories of the model in the swing phase. . . . .	21
3.7	Time proportion under spinal cord control over the swing cycle. . . . .	22
3.8	Time history of the kinematics of the body during the swing phase. . . . .	22
A.1	Spinal cord proportion of the other four trials with different initialization . . . . .	28



# List of Tables

3.1	Time proportion of each controller within 2 seconds before (shaded) and after external disturbances . . . . .	18
A.1	Dynamic parameters of the body segments . . . . .	27
A.2	Muscle parameters . . . . .	27
A.3	Brain controller parameters . . . . .	28



# Chapter 1

## Introduction

The spinal cord plays a vital role in the control of mammalian locomotion. Traditionally viewed as a hardwired relay system, more recent research indicates that the spinal cord is able to adapt, learn and reorganize locomotion control. Early evidence for this remarkable plasticity dates back to the 1980s when Forsberg and colleagues discovered that kittens whose spinal cord had been severed from the brain still learn locomotion skills when exposed to gait training [1]. Later on, similar outcomes have been documented for adult spinalized cats and rats [2, 3, 4, 5]. Similarly, spinal plasticity has been identified in humans. Examples include the observation of changes in synaptic transmission in the human spinal cord due to skill training [6, 7, 8], direct modulation of spinal reflexes through operant conditioning [9, 10, 11], and more generally, the observation of gait rehabilitation in patients with spinal cord injury [12, 13, 14, 15].

While the evidence for the spinal cord's ability to learn and adapt control is mounting, the neural mechanisms that underlie this plasticity are only vaguely understood. For instance, using neuroimaging techniques, Vahdat and colleagues found that during motor sequence learning of the upper limbs, neural activity shifts over time from brain areas to the spinal cord [16]. This observation broadly suggests that the underlying neural mechanisms include a transfer of control from the brain. More specifically, Landelle and colleagues propose that the increase in spinal cord activity during learning is linked to a decrease in presynaptic inhibition of motor neurons over time [17]. Probing the spinal circuitry involved in plasticity more directly,

## 1. Introduction

Brooke and Zehr observed a decrease in the H-reflex gain of the soleus muscle (SOL) with an increase in the frequency of rhythmic movements, suggesting an adaptive gain control due to Ia presynaptic inhibition [18]. More closely related to learning, Nielsen and colleagues demonstrated that such presynaptic inhibition of Ia afferent terminals plays a crucial role in training the co-contraction of antagonist muscles for maintaining joint stability [19]. Furthermore, Thompson and colleagues concluded from experiments on reflex operant conditioning that motor learning should comprise both, task-dependent adaptation associated with cortical and sub-cortical activity and more long-term changes in the spinal cord involving the firing threshold of motor neurons or interneuron activation [20, 21]. Overall, the knowledge gained from these and similar experimental studies so far provides only a vague and fragmentary picture of the explicit mechanisms that make up spinal plasticity at the circuit level.

Complementing experimental studies, computational and robot models have been developed to gain a more explicit, mechanistic understanding of how the circuits of the spinal cord could adapt and learn. For instance, Enander and colleagues [22] recently explored with a template neuromuscular model if the typical connectivity patterns observed in the spinal cord could arise from Hebbian learning at its neural synapses instead of being predefined genetically in early development. With a more realistic neuromuscular model of arm reaching, Verduzco-Flores and De Schutter [23] showed how differential Hebbian learning among neural synapses across the cortex and spinal cord could transform arm movements from initial motor babbling to reaching specific targets after training. Closer to human locomotion, Manoonpong and colleagues demonstrated with a robot biped model how differential Hebbian learning at the equivalent motor neurons of the model’s spinal control can automatically adapt the control of walking between level and sloped ground [24]. Motivated by the observed shift in activity from the brain to the spinal cord during motor skill learning [16, 17], we recently showed with a neuromuscular model of human hopping how the control of a locomotion behavior may be transferred between brain and cord by heterosynaptic learning at the synapses of spinal reflex circuits [25]. Although this model provided an initial step in this direction, it also pointed out shortcomings of our proposed learning circuitry. It can not simultaneously learn multiple behaviors, such as the basic motor pattern of hopping and the recovery of balance after disturbances. Nor can the brain control activity ramp down with training progress in this model.

Here, we propose a possible learning framework at the spinal cord level to address the potential improvements from our previous work [25]. The model aims to simultaneously learn and adapt to different behaviors, namely hopping and disturbance rejection, at different frequencies. Drawing inspiration from Haruno’s work on controller selection [26], we incorporate multiple spinal cord controllers and a responsibility network to enable automatic selection among them. Moreover, we introduce a brain-spinal cord switch to actively engage the brain and the learning process. The methods of controller selection and adaption are inspired by Haruno et al. [26]. In the rest of the thesis, [chapter 2](#) documents our system, modeling, and learning framework of control transfer. We extended the model to a complete single-legged hopper with a trunk, actuated by nine muscles. Additionally, to better simulate the process of transferring control from the brain to the spinal cord, we propose an active switch mechanism, in addition to the multiple spinal cord controllers, to spontaneously switch to the spinal cord or enable learning at the spinal cord during training. In [chapter 3](#), we present the learned controllers. We find that the learned spinal cord controller can coordinate multiple controllers and switch among them based on contextual signals to control most of the hopping motion. We also analyze the functional role of the controller learned at the spinal cord. [chapter 4](#) discusses our results and possible improvements in future work.

## *1. Introduction*

# Chapter 2

## Methods

As a template for human locomotion, we focus on bipedal hopping in place for the goal behavior to be learned by the spinal cord control circuits. Similar to walking and running, this behavior requires separate stance and swing controls with a focus on generating leg rebound in stance, placing the feet in swing, and maintaining trunk balance throughout. In contrast to walking and running, however, in bipedal hopping the human musculo-skeletal system can be simplified to a single kinematic chain with correspondingly fewer muscle actuators. We first describe the musculo-skeletal mechanics of the model and then detail its neuromuscular control and learning.

### 2.1 Musculo-Skeletal Mechanics

The mechanics of human hopping in place are represented by a four-segment chain modeling the trunk, thighs, shanks, and feet in the sagittal plane (Fig. 2.1). The segments are connected by revolute hip, knee, and ankle joints, which are actuated by nine Hill-type muscles representing the soleus (SOL), tibialis anterior (TA), gastrocnemius (GAS), vasti group (VAS), biceps femoris short head (BFsH), hamstring (HAM), rectus femoris (RF), gluteus (GLU), and hip flexors (HFL). Each Hill-type muscle produces a force  $F_m(l_m, v_m, s_m)$  as a function of its length ( $l_m$ ), velocity ( $v_m$ ) and muscle stimulation ( $s_m$ ), and contributes to the torque of any joint  $j$  it spans via

## 2. Methods

the moment arm  $r_j^m(\theta_j)$ ,

$$\tau_j = \sum_m r_j^m(\theta_j) F_m .$$

The specific muscle and moment arm implementations are provided in [25, 27]. Similarly, the muscle and segment parameters were taken from these previous implementations with modifications made to mass( $m_i$ ), inertia( $I_i$ ), and muscle parameters to account for bipedal hopping (see [table A.1](#) in [appendix A](#) for detail). Finally, the resulting segment chain dynamics are governed by

$$\mathbf{M}(\boldsymbol{\theta})\ddot{\boldsymbol{\theta}} + \mathbf{C}(\boldsymbol{\theta}, \dot{\boldsymbol{\theta}})\dot{\boldsymbol{\theta}} + \mathbf{N}(\boldsymbol{\theta}) + \mathbf{J}^T(\boldsymbol{\theta})\mathbf{F}_{grf} = \boldsymbol{\tau} ,$$

where  $\mathbf{M}$ ,  $\mathbf{C}$ , and  $\mathbf{N}$  are the mass matrix, coriolis matrix, and the gravitational term, respectively, and  $\mathbf{F}_{grf}$  is the ground reaction force in stance mapped into joint contributions via the Jacobian  $\mathbf{J}$ . Note that the model only considers forefoot hopping with a single contact point at the toe of the foot segment.

## 2.2 Brain Reference Controller

In our previous work on spinal control learning [25], we followed the idea that the learning happens by a transfer of control from the brain to the cord. In keeping with this overall idea, we here assume the model already possesses a brain reference controller that generates hopping while recovering from push disturbances. Whether this brain controller is physiologically plausible does not matter, as it really just serves as a reference for spinal control learning.

The implemented brain controller distinguishes between stance and flight phases [Fig. 2.2](#). In stance, its control goals are (i) to generate a leg rebound motion implemented by soft proportional controls

$$\tau_j^{st} = k_{pj}^{st} (\phi_j^{*,st} - \phi_j), \quad j = \{k, a\}$$

about reference angles  $\phi_j^{*,st}$  for the knee and ankle that correspond to an outstretched leg configuration, and (ii) to balance the trunk at a reference pose  $\theta^*$  of the lean angle



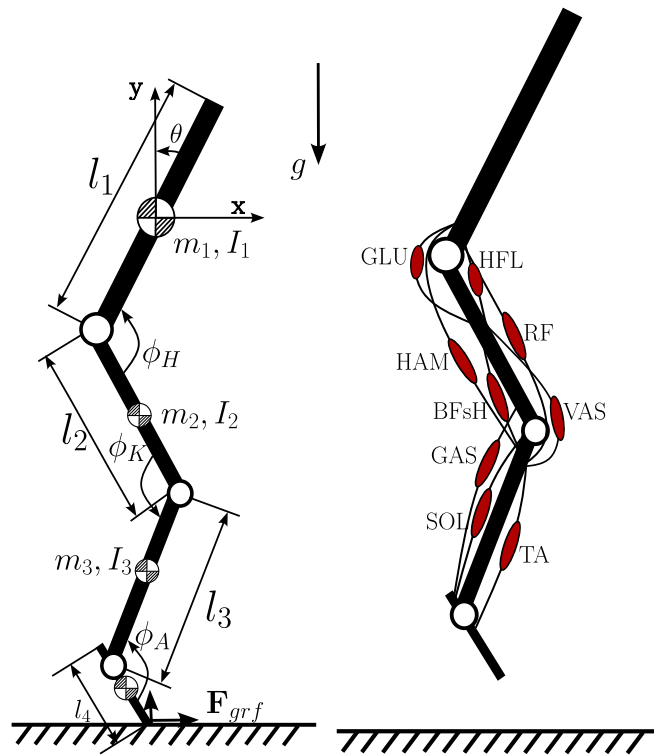


Figure 2.1: Kinematics of the model and muscles involved.

## 2. Methods

$\theta$  implemented with a proportional-derivative control

$$\tau_h^{st} = k_{ph}^{st} (\theta^* - \theta) - k_{dh}^{st} \dot{\theta}.$$

In flight, the goal of the brain controller is to place the leg such that the trunk of the model will maintain or return to the origin ( $x^* = 0$ ) in the subsequent stance. To this end, the controller tracks desired joint angles  $\phi_j^*$  with

$$\tau_j^{fl} = k_{pj}^{fl} (\phi_j^{*,fl} - \phi_j) - k_{dj}^{fl} \dot{\phi}_j, \quad j = \{a, k, h\}$$

where  $\phi_h^{*,fl}$  and  $\phi_k^{*,fl}$  vary over the course of flight. Specifically, these angles vary according to

$$\begin{aligned} \phi_h^{*,fl} &= \phi_h^{\text{ref}} + \theta - \arcsin(x_{\text{td}}) \\ \phi_k^{*,fl} &= \phi_k^{\text{ref}} + k_{xk} x_{\text{td}} \end{aligned}$$

with  $x_{\text{td}}$  describing a desired horizontal touch-down position

$$x_{\text{td}} = k_x (x^* - x) + k_{\dot{x}} \dot{x} - \frac{l_1}{2} \theta.$$

The desired touch-down position is based on a proportional-derivative feedback of the trunk horizontal position from the origin (first two terms) corrected by the current trunk lean (third term).

In both stance and flight, the desired joint torques  $\tau_j$  are converted into stimulations  $s_m^b$  the brain controller sends to the muscle actuators of the model. For the monoarticular muscles (SOL, TA, VAS, BF<sub>s</sub>H, GLU, HFL), the torques convert directly into stimulations,

$$s_m^b = \begin{cases} \max(0, \tau_j), & m = \{\text{SOL, VAS, GLU}\} \\ -\min(\tau_j, 0), & m = \{\text{TA, BF}_s\text{H, HFL}\} \end{cases}$$

For the biarticular muscles (GAS, HAM, and RF), the stimulations are proportioned

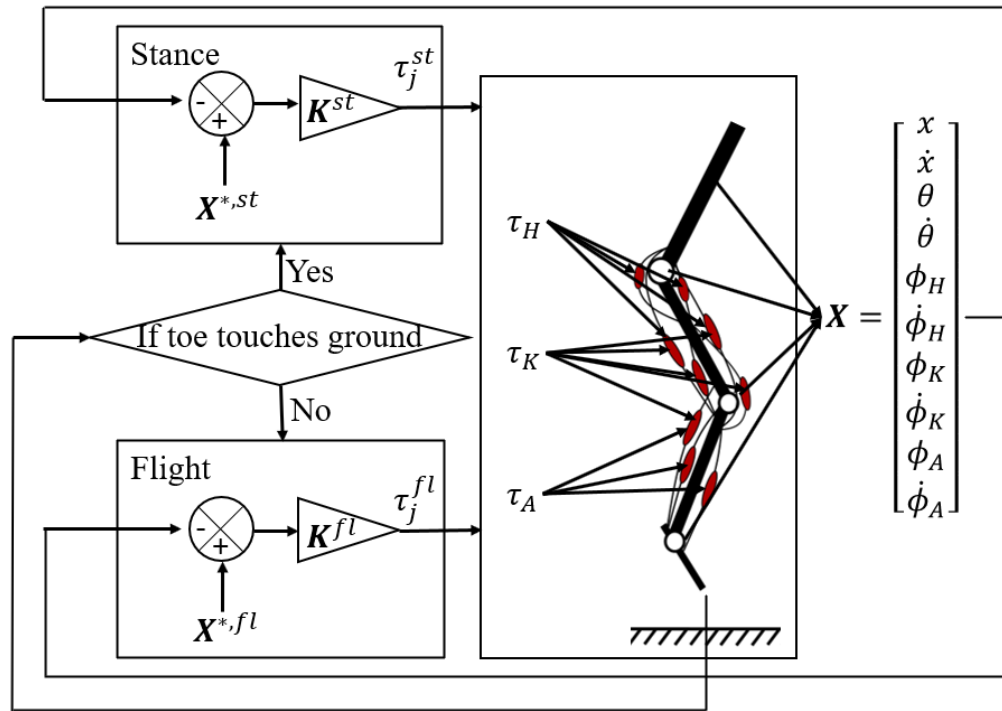


Figure 2.2: Schematic of the brain controller

to the torques of the joints that these muscles span,

$$\begin{aligned} s_{\text{GAS}}^b &= \max(0, k_{\text{GAS},a}\tau_a - k_{\text{GAS},k}\tau_k) \\ s_{\text{HAM}}^b &= \max(0, k_{\text{HAM},h}\tau_h - k_{\text{HAM},k}\tau_k) \\ s_{\text{RF}}^b &= \max(0, k_{\text{RF},k}\tau_k - k_{\text{RF},h}\tau_h) \end{aligned}$$

These stimulation signals are sent to the spinal cord with a 15 ms delay to account for the time it takes these signals to travel from the brain to the alpha motoneurons ( $\alpha$ MNs) of the leg muscles in the lumbar spinal cord. Note that, as is common in neuromuscular models with Hill-type muscles, the resulting  $\alpha$ MN outputs are saturated between zero and one, and then further time-delayed before they reach the muscles (compare section 2.3).

The gains and reference angles of the brain controller are optimized with the covariance matrix adaptation evolutionary strategy (CMA-ES [28]), and the resulting controller (parameters reported in table A.3) lets the model achieve steady hopping with about 4 cm jumping height while recovering from random, horizontal pushes to the trunk center of mass of up to 100 N m applied every five to ten seconds.

## 2.3 The spinal cord controller network

The spinal control circuitry combines elements of [25] and [26] (Fig. 2.3). Similar to [25], it consists of basic interneuron networks (index  $k$ ) that for each muscle  $m$  generate outputs

$$y_m^k(t) = \sum_{i=1}^n w_{m,i}^k x_i(t - \Delta t_i)$$

that integrate time-delayed sensory signals  $x_i(t - \Delta t_i)$  weighted by the synaptic strengths  $w_{m,i}^k \geq 0$ .  $x_i$  refers to proprioceptive signals from muscles and vestibular feedback. For each muscle, there are six proprioceptive signals, which are excitatory and inhibitory force, length, and velocity. For vestibular feedback, there are twelve signals in total, which are the positive and negative portion of  $\theta$ ,  $\dot{\theta}$ , and  $\ddot{\theta}$ , acting as either excitatory or inhibitory feedback. However, in contrast to [25], there are

multiple copies of these basic networks and the amount by which each individual network's output drives the muscle stimulation generated by the  $\alpha$ MN is determined by a responsibility  $\rho^k$ .

$$s_m^r(t) = \sum_{k=1}^c \rho^k(t) s_m^k(t)$$

$$\rho^k(t) = \sum_{i=1}^n w_j^k x_i(t - \Delta t_i)$$

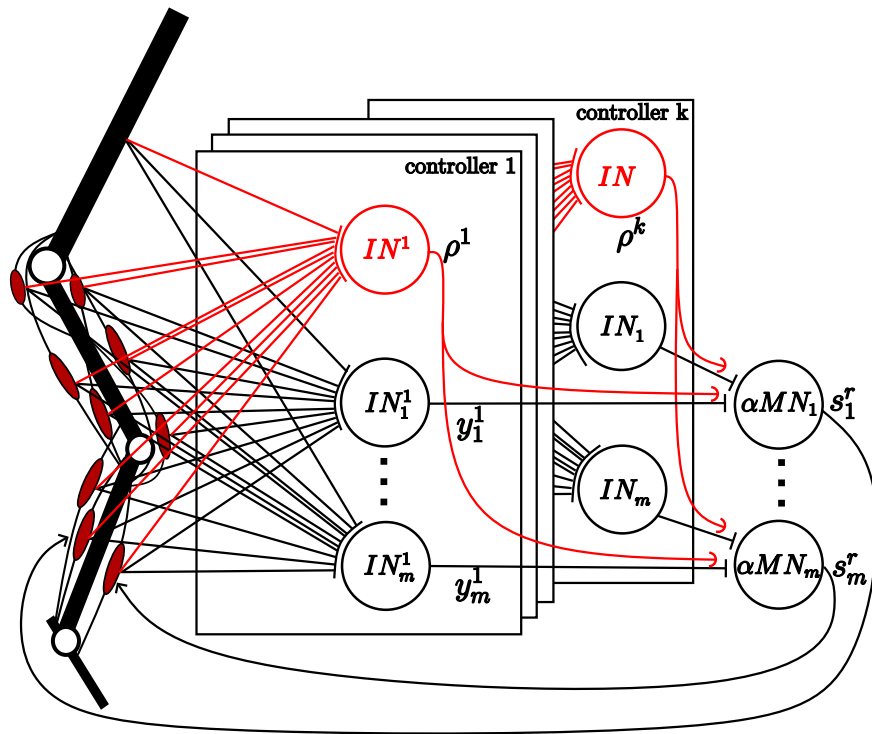


Figure 2.3: Spinal cord controller structure

### 2.3.1 Spinal cord learning

The learning rule of synaptic weights combines the rule from the previous work [25] and [26]. As the spinal cord determines the final stimulation based on multiple

## 2. Methods

networks and their corresponding responsibilities, we categorize the synaptic weights into controller weights ( $w_{m,i}^k$ ) and responsibility weights ( $w_i^k$ ). To update the controller weights at time  $t$ , the error

$$e_m^k(t) = s_m^b(t - \Delta t_b) - y_m^k$$

between the stimulation from the brain and the output  $y_m^k$  from all responsible networks ( $\rho_{ref}^k \neq 0$ ) are used to update the corresponding synaptic weights.

$$\dot{w}_{m,i}^k = \mu(\rho_{ref}^k e_m^k(t) x_i(t - \Delta t_i) - \lambda w_{m,i}^k)$$

The reference responsibility signal ( $\rho_{ref}^k$ ) is determined through the maximum likelihood principle. To identify which network should be used, the prediction errors ( $e_m^k(t)$ ), are used to calculate the likelihood  $l^k$ , after being added with Gaussian noise with standard deviation  $\sigma$ [26].

$$l^k = \frac{1}{\sqrt{2\pi\sigma^2}} \exp\left(-\frac{\sum_{m=1}^9 (e_m^k)^2}{2\sigma^2}\right)$$

The reference responsibility is the normalized product of the likelihood  $l^k$  and the predicted responsibility  $\rho^k$ .

$$\rho_{ref}^k = \frac{\rho^k l^k}{\sum_{j=1}^4 \rho^j l^j}$$

Other than determining the contribution of each network during learning, the reference responsibility signal is also used to train the responsibility synapse.

$$\dot{w}_i^k = \mu\left((\rho_{ref}^k - \rho^k) x_i(t - \Delta t_i) - \lambda w_i^k\right)$$

Specifically for our project, four controllers are used for the stance phase and four for the swing phase. The learning rate  $\mu$  is  $0.15s^{-1}$  and the decay rate  $\lambda$  is 0.01. A small decay rate allows the unused controllers, of which  $\rho^k = 0$ , to decay slowly and resulted in having more chance of being used. The full learning schematic is as shown in Fig. 2.4. The black lines refer to the update loop related to the controller synapses and the red lines refer to that of responsibility synapses.

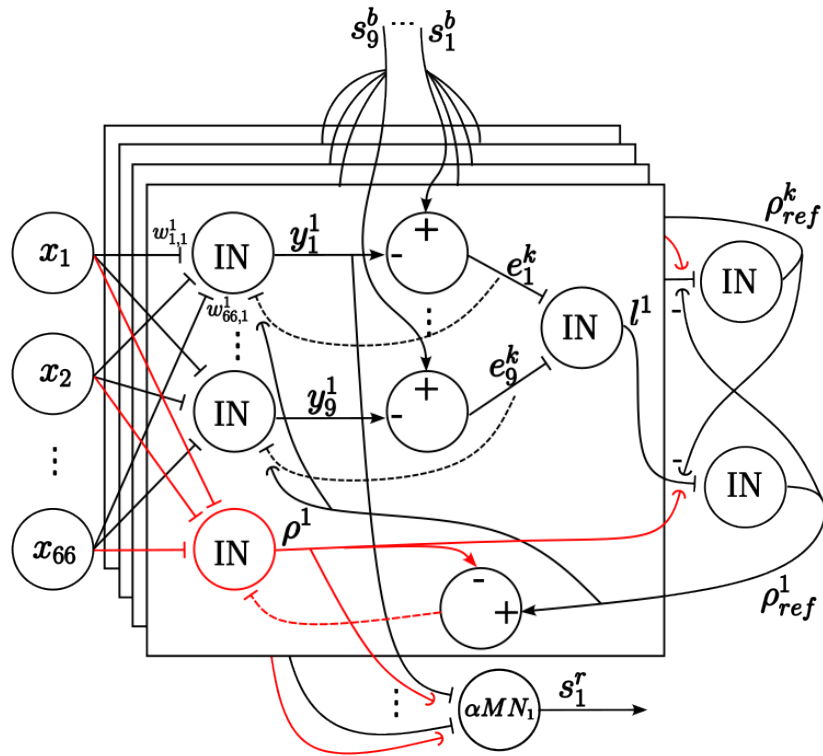


Figure 2.4: Learning framework

### 2.3.2 Switch mechanism between brain and spinal cord

The switching mechanism between the brain and spinal cord is a sliding threshold. As the learning process requires the supervision from brain, it is energy inefficient to learn all the time. Hence, we propose to use a sliding threshold of biological signals to engage the brain for controlling and learning. The signal used in the swing phase is the angular acceleration of the trunk  $\ddot{\theta}$ , and that in the stance phase is the linear acceleration of the trunk  $\ddot{x}$ . These two signals are predetermined by running correlation tests between the mean absolute error between  $s_m^b$  and  $s_m^r$  and possible biological signals. The stimulation received by the muscle at time  $t$  is generated by the spinal cord, if the measured biomechanics signal is within the threshold, otherwise by the brain.

$$s_m(t) = \begin{cases} s_m^r(t - \Delta t_m) & |\ddot{\theta}| < \tilde{\theta}, \text{ in swing} \\ s_m^b(t - \Delta t_m - \Delta t_b) & |\ddot{\theta}| \geq \tilde{\theta}, \text{ in swing} \\ s_m^r(t - \Delta t_m) & |\ddot{x}| < \tilde{x}, \text{ in stance} \\ s_m^b(t - \Delta t_m - \Delta t_b) & |\ddot{x}| \geq \tilde{x}, \text{ in stance} \end{cases}$$

As the training progress, the thresholds are updated based on past performance,

$$\begin{aligned} \tilde{\theta} &= \tilde{\theta} + \eta dt \\ \tilde{x} &= \tilde{x} + \eta dt \end{aligned}$$

where  $\eta$  is the rate of change of the threshold. During the learning process, when the model consistently uses the spinal cord for a cumulative 200 steps, the threshold values ( $\tilde{\theta}$  and  $\tilde{x}$ ) will increase, resulting in a tendency to use the spinal cord more. However, we identified that the learning result of the spinal cord can be sensitive to the choice of  $\eta$ . Larger  $\eta$  may result in worse training results due to consistent falling, while smaller  $\eta$  may cause the training time to be significantly longer.



# Chapter 3

## Results

The model was simulated in MATLAB starting from the initial apex. All weights were randomly initialized, and the simulation was stopped when the spinal cord proportion stopped growing or started dropping while the threshold kept increasing.

### 3.1 Does the proposed framework learn?

The proposed learning framework shows the learning and the adaption of the spinal cord. We run the training process five times with different initializations. The stopping criterion is when the time proportion of spinal cord control stops increasing while increasing the thresholds. Fig. 3.1 has shown the time proportion of spinal cord control over the whole training of one experiment. The red dotted line is the final mean spinal cord proportion. The spinal cord proportion during training of other trials can be found in [appendix A](#). At the end of the five experiments, on average 99.5% of the time, the stimulations received by the muscles in the stance phase are generated from the spinal cord, which indicates that the stance control is transferred to the spinal cord successfully. In the swing phase, however, it ends up using on average 85% of the time. In addition, over the five different experiments, the spinal cord networks all end up using three controllers in the stance phase and two controllers in the swing phase. As the activation pattern of each controller follows a similar trend through every step in five experiments Fig. 3.2(a), we name them controller st 1, controller st 2, and controller st 3 and controller sw 1 and controller

### 3. Results

sw 2.

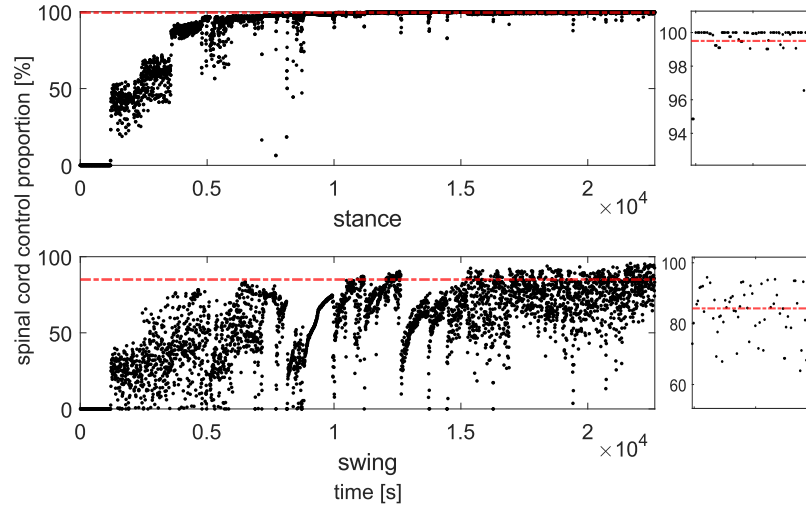


Figure 3.1: Spinal cord proportion over training.

Moreover, the majority of the controller weights converge to similar distributions with some variations in magnitude. Fig. 3.2(b) shows the result of the principal component analysis(PCA) of all five trials. The y-axis in this figure is the cumulative explained variance(CEV). As shown in this figure, in both the stance and swing phase, the first principal component can explain at least 70% of the variance (controller st 3 and controller sw 2), and at most 90% of the variance (controller st 1 and controller sw 1). This shows that the resulting networks converge to a similar distribution. In addition, a coefficient of variation(CV) test is also done to measure the variation of the individual weight values. Fig. 3.2(c) shows the cumulative percentage of active pathways which has a coefficient of variation(CV) less the value on the x-axis. In this figure, we only consider the weights that contribute to more than 10% of the stimulation. The relative trend among the controllers also aligns with the PCA result. However, the absolute CV value shows that the individual values vary from trial to trial.

## 3.2 Functional roles of each controller

The functionality of each controller is distinguished based on behavior groups that are not considered external disturbances. As shown in Table 3.1, the average respon-

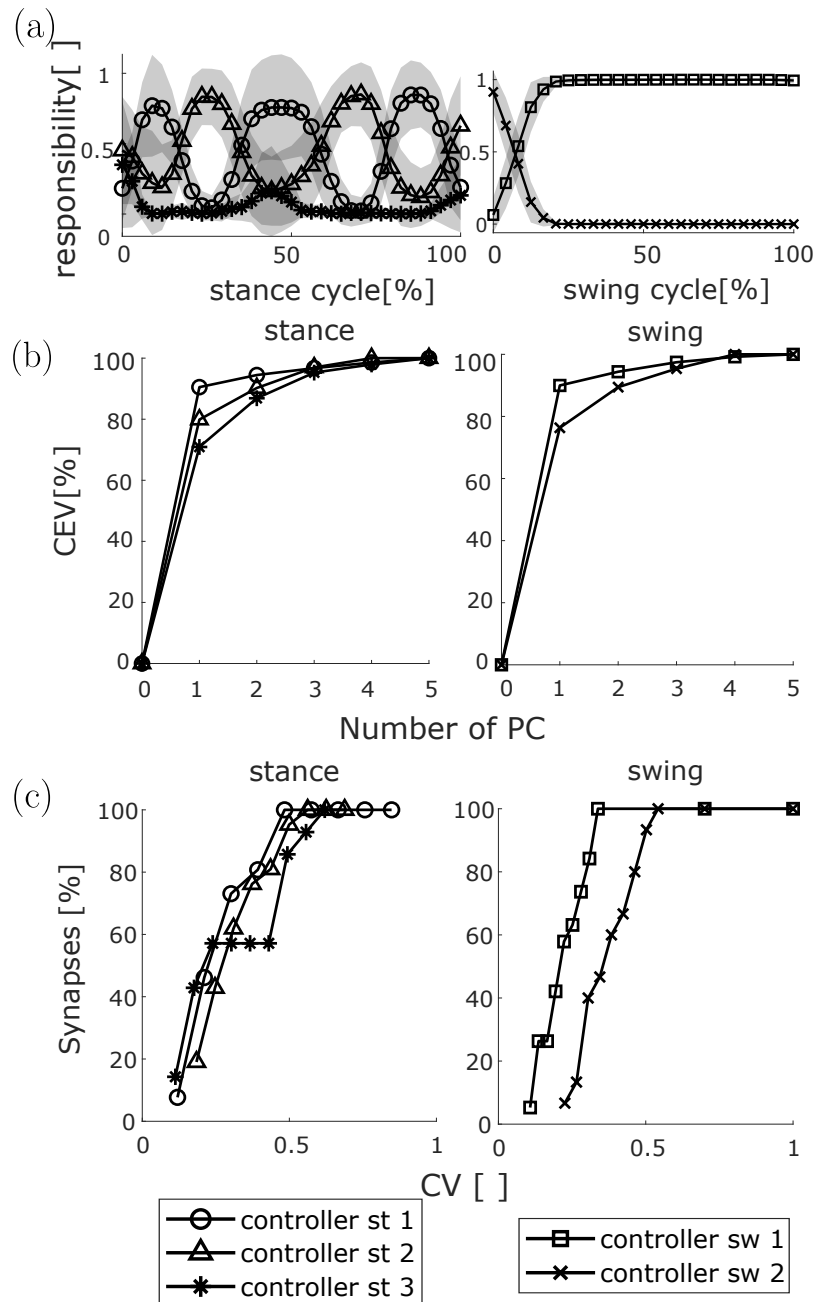


Figure 3.2: Weights at the spinal cord converge to similar controllers. (a) Activation patterns of controllers over the stance and swing cycle. (b) PCA analysis of all weights from five trials. (c) Cumulative percentage of the active pathways

### 3. Results

sibility values of each controller before and after applying disturbances do not differ significantly.

	controller 1		controller 2		controller 3	
stance	45.2%	43.7%	47.4%	48%	6.9%	7.7%
swing	80.87%	80.87%	6%	5.9%		

Table 3.1: Time proportion of each controller within 2 seconds before (shaded) and after external disturbances

To gain a deeper understanding of the functional role of each controller, we plot the pathways with a stimulation contribution of more than 10% on average and a coefficient of variation of less than 0.3. The resulting average stimulation contributions are summarized in Figures 3.3 and 3.5.

#### 3.2.1 Stance phase

The functional roles of controller st 1 and controller st 2 are similar, as they are responsible for braking, pushing up, and trunk stabilization. The common significant reflex groups in both controller st 1 and controller st 2 include positive length ( $L^+$ ) and velocity ( $V^+$ ) feedback among SOL, GAS, and VAS, which are commonly interpreted as braking while landing. The positive force ( $F^+$ ) feedback facilitates pushing up. Another shared reflex group involves pathways from the vestibular system to hip extensors in controller st 1, and to hip flexors in controller st 2. These pathways help stabilize the trunk during stances. Additionally, heteronymous pathways across joints, such as from BF<sub>s</sub>H  $V^+$  to HAM and GLU to extend the hip together with the knee, and from HAM  $F^+$  to VAS to stiffen the knee joint.

In contrast, controller st 3 is not active in every stance. Figure 3.4 illustrates the average posture of the model under controller 3 during early stance and mid stance. The blue starred lines represent the mean trajectories under controller st 3, while the red dotted lines show the mean trajectories under other controllers. In mid to late stance, it plays a role in handling postures when the trunk is significantly leaning forward, the knee joint tends to overextend, and the ankle joint is compressed. Controller st 3 facilitates pushing up and straightening the trunk by activating all the extensor muscles using feedback from vestibular pathways and BF<sub>s</sub>H  $L^+$ , as shown

in Figure 3.3. However, this scenario is relatively rare, occurring only five times out of more than five hundred hops.

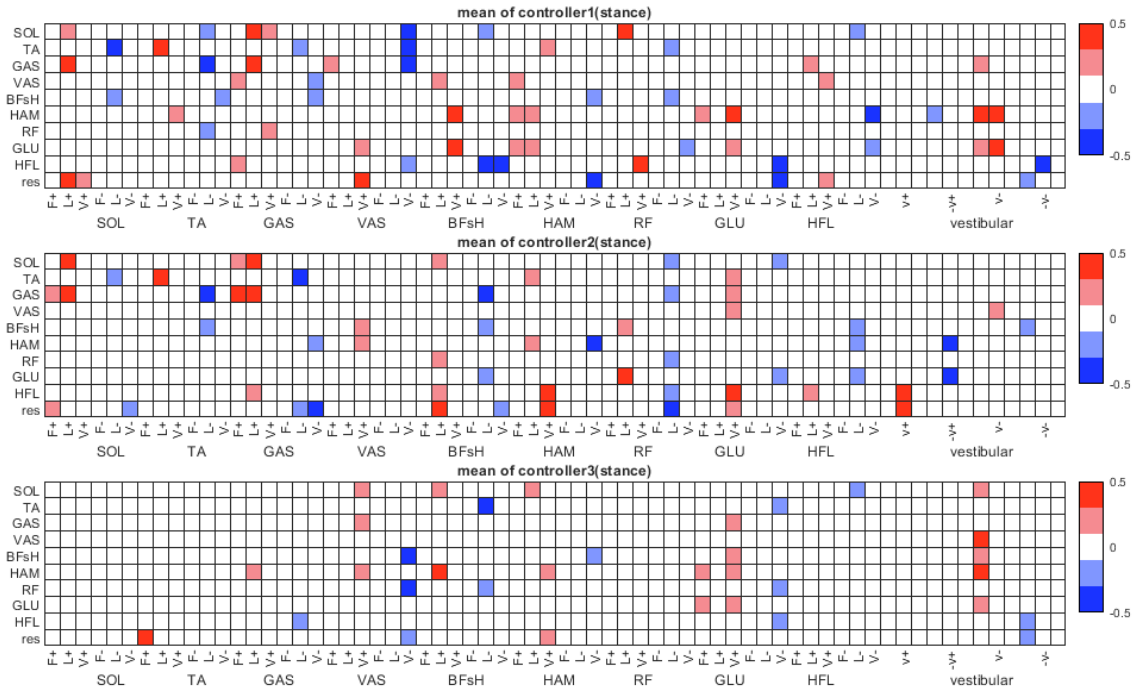


Figure 3.3: Average stimulation contribution in stance phase

### 3.2.2 Swing phase

In the swing phase, controller sw 1 employs vestibular feedback to adjust the touch-down position closer to the center of gravity, as demonstrated in the kinematic plot (Fig. 3.6). Fig. 3.5 illustrates the average stimulation contribution during the swing phase. The alternating heteronymous 1a pathways among HAM, GLU, and HFL are utilized by controller sw 1 to ensure smooth and gradual movements of the hip joint. We believe that these reflexes contribute to adjusting leg placements and a smoother transition to stance. Meanwhile, controller sw 2 is responsible for adjusting the trunk position during the initial swing. As the stance phases always end with a positive acceleration of the trunk, controller sw 2 utilizes the pathways from the positive velocity of the trunk and 1b pathway of itself to activate the hip flexor muscle to the maximum.

### 3. Results

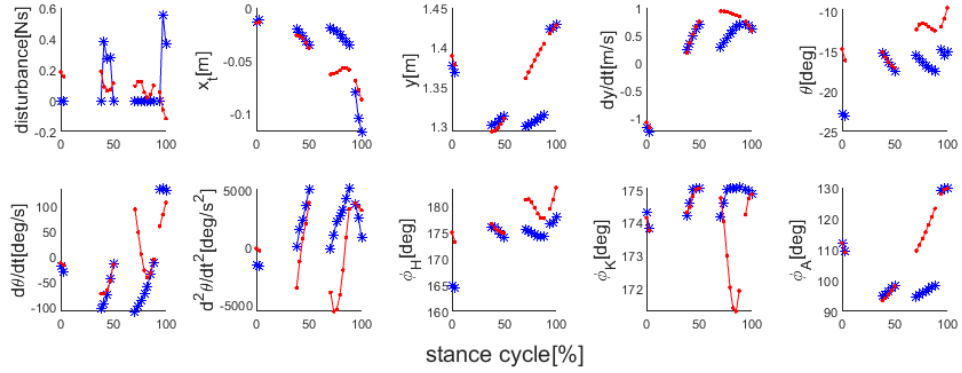


Figure 3.4: Average kinematics of the body.

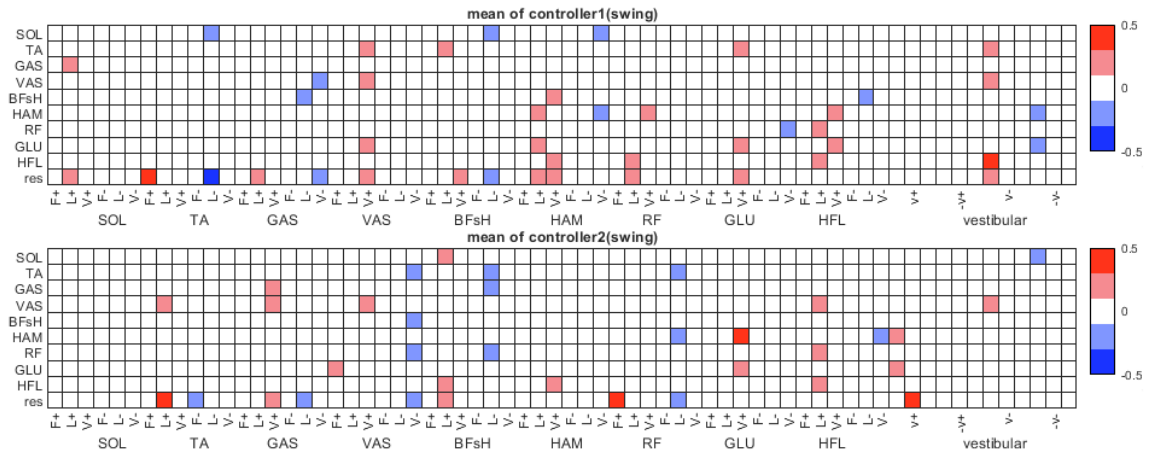


Figure 3.5: Average stimulation contribution in swing phase

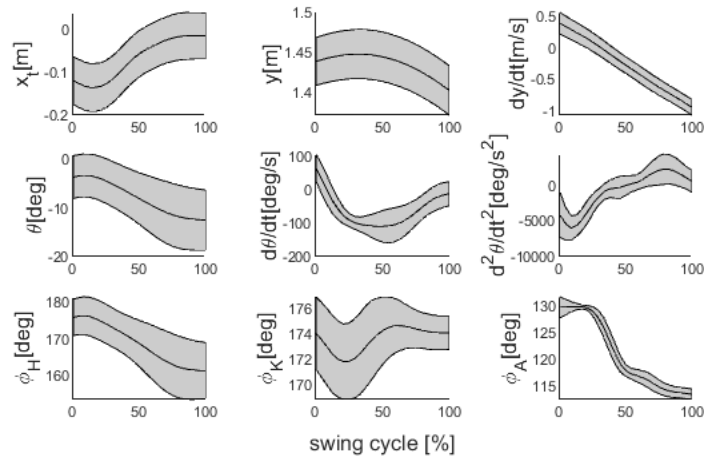


Figure 3.6: Average kinematic trajectories of the model in the swing phase.

### 3.3 Reason for switching back to the brain control

The spinal cord's inability to function at 100% on its own leads to switching back to brain control, triggered by large trunk angular acceleration, as determined by the switching criteria used during the training process. This switch typically occurs during the first half of the swing phase, with a concentration in the early swing, as shown in Fig. 3.7 from 4% to 8%. The shaded area represent the standard deviation. The sudden drop in spinal cord control proportion from 4% to 8% of the swing cycle can be attributed to the switch between the two controllers, causing overstimulation of the hip flexors and less stimulation of the hip extensors, resulting in a drop in the knee angle at that particular time point (Fig. 3.8).

However, in the other portion of the swing cycle, the reasons causing large trunk angular velocity that lead to switching back to brain control are not yet clearly understood. Further investigations are required to gain insights into the specific factors influencing this behavior.

### 3. Results

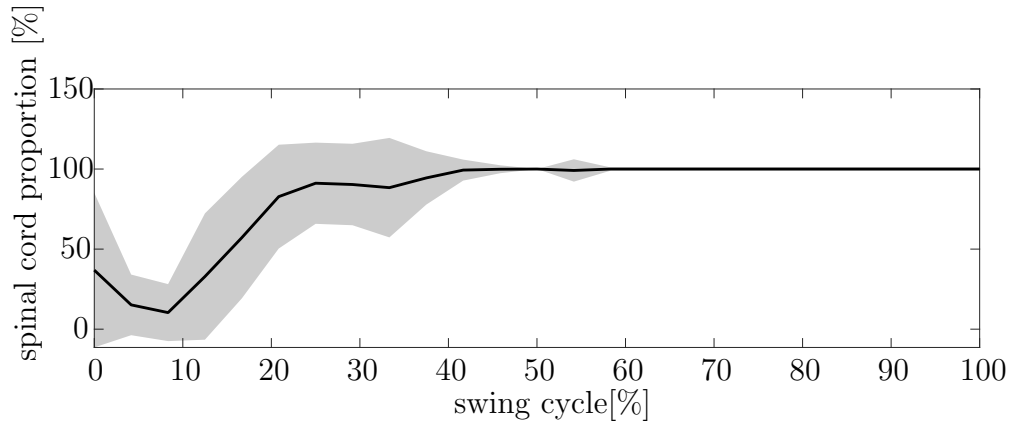


Figure 3.7: Time proportion under spinal cord control over the swing cycle.

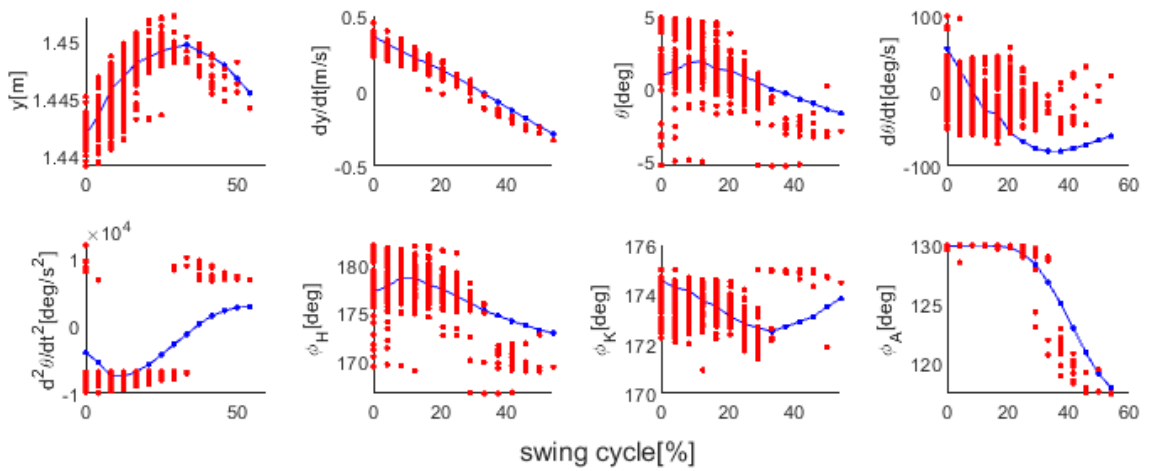


Figure 3.8: Time history of the kinematics of the body during the swing phase.



# Chapter 4

## Discussion

The results suggest a potential learning framework for the spinal cord to acquire multiple locomotion behaviors at different frequencies. The process of transferring control has been demonstrated in both physiological experiments [16] and neuromuscular modeling [25]. In this study, we further explored the capability of simultaneous transfer and self-identification of multiple controllers through this process. The structure of the spinal cord circuitry used in this study aligns with the findings from Hultborn [29] and Rossignol’s group [30].

Although the final spinal cord proportion, as shown in Fig. 3.1, is not hundred percent over the entire gait cycle, the model has another layer of switching mechanism to engage the brain control, which is also a possible mechanism that exists in human locomotion. However, the switching mechanism is oversimplified by using a single biomechanical signal each for the stance and swing phases.

Our results also suggest that the separation of the controllers may not be solely related to disturbances, as expected from the previous work by Sar and Geyer [25]. As shown in Table 3.1, the average time proportion of each controller before and after external disturbances barely differs from each other. This suggests that the learned control structure is capable of dealing with disturbances in a different way. It may also be due to the fact that the hopping motion is not strictly periodic even without external disturbances. Since the spinal cord controller is not a perfect replication of brain control, non-periodic postures can be induced frequently during both training and testing. Thus, minor disturbances that do not cause significant

posture differences, as shown in Figure 3.4, do not require a separate controller with different reflex pathways. Similarly, in the work of Song and Geyer [31], the generated spinal cord circuitry has the ability to reject disturbances.

### 4.1 Future work

In addition, the reflexes learned through this network contain common reflex groups that have been identified, such as the reflex pathways related to ankle and knee extensors for braking and pushing up, as well as the 1a pathways across joints and between antagonist muscles for muscle synergies. However, even though we have eliminated many pathways using thresholding of coefficient of variation and fraction of stimulation contribution, there are still pathways that are not documented in the previous literature [25][32]. The specific functional roles of these pathways remain unclear. This could be partly attributed to the oversimplified brain controller. As the parameters used in the brain control are obtained through a genetic algorithm, the stimulation pattern can differ significantly from that of a real human. For example, when HFL and VAS are co-activated during swing and stance, it is possible to use RF instead of activating two separate muscles. However, the optimization results in not activating RF but saturating the stimulations of HFL and VAS. Hence, one of the future works of this study is to optimize the brain controller to align with human experimental results. Furthermore, the current learning framework only contains linear relationships, which may cause imperfections in learning results, as shown in the final spinal cord proportion. Therefore, adding non-linearity is another possible area for future work.

# Chapter 5

## Conclusions

Learning behaviors with different frequencies simultaneously is a desirable feature of the human spinal cord. Our model, inspired by [26], describes a possible mechanism that could achieve simultaneous learning of multiple spinal cord controllers and automatically switch between them. Moreover, our model also adopts an additional switching mechanism between the brain and the spinal cord. Instead of completely cutting off the connection between the brain and the spinal cord after learning, this switching mechanism allows the model to re-engage the brain to facilitate further adaption. In addition, we also discuss the functional roles of each controller learned with an explicit analysis of some important reflex groups, though leaving the uncommon pathways. The proposed model sheds light on the possible framework of the human spinal cord to learn behaviors with different frequencies simultaneously and adapt dynamically, offering insights for future research in the field of neural control and rehabilitation.

## 5. Conclusions

# Appendix A

## Modeling parameters

	Mass[kg]	Inertia[kg/m <sup>2</sup> ]	Length[m]
Trunk	53	3	0.6
Thigh	17.4	0.3	0.5
Shank	6.4	0.1	0.1
Foot	1.9	0.01	0.01

Table A.1: Dynamic parameters of the body segments

	SOL	TA	GAS	VAS	BFsH	HAM	RF	GLU	HFL
$F_{max}$ [N]	8000	1600	3000	12000	700	6000	2400	3000	4000
$v_{max}$ [m/s]	6	12	12	12	12	12	12	12	12
$l_{optV}$ [m]	0.04	0.06	0.05	0.08	0.12	0.10	0.08	0.11	0.11
$l_{slack}$ [m]	0.26	0.24	0.40	0.23	0.10	0.31	0.35	0.13	0.10
$\epsilon_{refV}$	0.04	0.04	0.04	0.04	0.04	0.04	0.04	0.04	0.04
$\Delta t$ to spinal cord [ms]	10	10	10	5	5	2.5	2.5	2.5	2.5
$\Delta t$ from spinal cord [ms]	10	10	10	5	5	2.5	2.5	2.5	2.5

Table A.2: Muscle parameters

A. Modeling parameters

stance	$K_{pH}$	$K_{pK}$	$K_{pA}$	$K_{dH}$	$\phi_K^*[deg]$	$\phi_A^*[deg]$	$\theta^*[deg]$
	3	0.8956	3	1.211	237.93	124.51	7.5
swing	$K_{pH}$	$K_{pK}$	$K_{pA}$	$K_{dH}$	$K_{dK}$	$K_{dA}$	$k_x$
	2.1984	0.0977	3	0.4823	0.0684	1.3817	0.01
	$k_{\dot{x}}$	$K_{xk}$	$\phi_H^*$	$\phi_K^*[deg]$	$\phi_A^*[deg]$		
	0.6781	2.5661	191.4177	185.1590	81.1420		
biarticular	$k_{GAS,a}$	$k_{GAS,k}$	$k_{HAM,h}$	$k_{HAM,k}$	$k_{RF,k}$	$k_{RF,h}$	
	1.4452	0	1.5	0	0	0	

Table A.3: Brain controller parameters

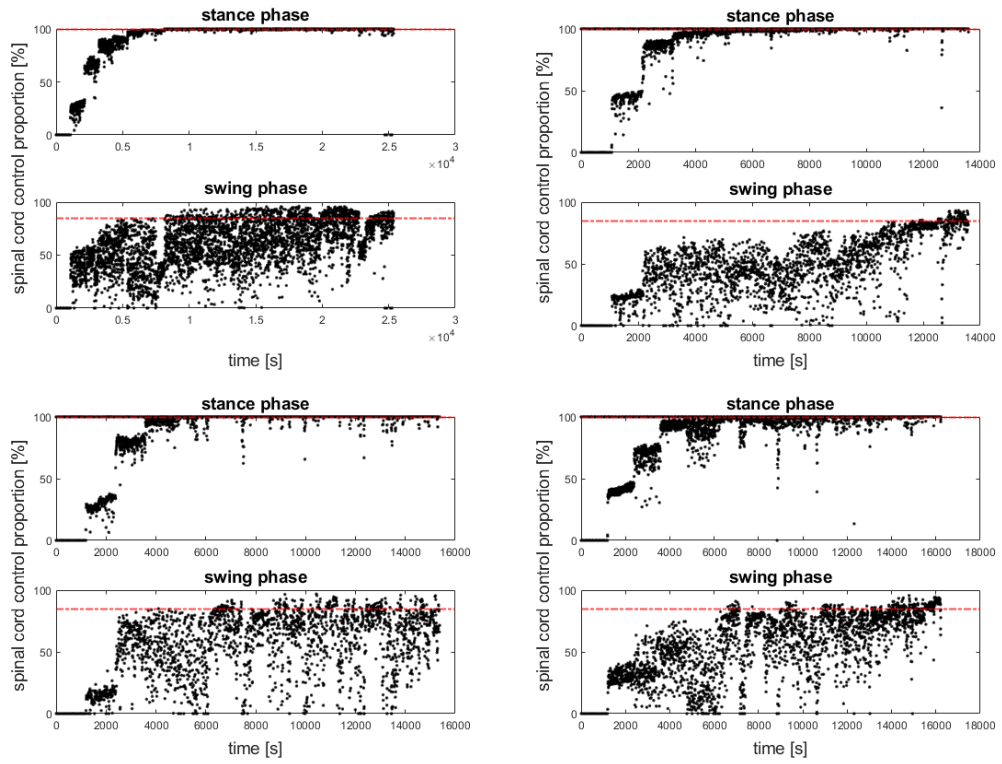


Figure A.1: Spinal cord proportion of the other four trials with different initialization

# Bibliography

- [1] H. Forssberg, S. Grillner, and J. Halbertsma, “The locomotion of the low spinal cat i. coordination within a hindlimb,” *Acta Physiologica Scandinavica*, vol. 108, no. 3, pp. 269–281, 1980. [1](#)
- [2] H. Barbeau and S. Rossignol, “Recovery of locomotion after chronic spinalization in the adult cat,” *Brain research*, vol. 412, no. 1, pp. 84–95, 1987. [1](#)
- [3] G. Courtine, Y. Gerasimenko, R. Van Den Brand, A. Yew, P. Musienko, H. Zhong, B. Song, Y. Ao, R. M. Ichiyama, I. Lavrov, *et al.*, “Transformation of nonfunctional spinal circuits into functional states after the loss of brain input,” *Nature neuroscience*, vol. 12, no. 10, pp. 1333–1342, 2009. [1](#)
- [4] R. Kawai, T. Markman, R. Poddar, R. Ko, A. L. Fantana, A. K. Dhawale, A. R. Kampff, and B. P. Ölveczky, “Motor cortex is required for learning but not for executing a motor skill,” *Neuron*, vol. 86, no. 3, pp. 800–812, 2015. [1](#)
- [5] S. Rossignol, “Plasticity of connections underlying locomotor recovery after central and/or peripheral lesions in the adult mammals,” *Philosophical Transactions of the Royal Society B: Biological Sciences*, vol. 361, no. 1473, pp. 1647–1671, 2006. [1](#)
- [6] A. Casabona, M. Polizzi, and V. Perciavalle, “Differences in h-reflex between athletes trained for explosive contractions and non-trained subjects,” *European journal of applied physiology and occupational physiology*, vol. 61, pp. 26–32, 1990. [1](#)
- [7] J. Nielsen, C. Crone, and H. Hultborn, “H-reflexes are smaller in dancers from the royal danish ballet than in well-trained athletes,” *European journal of applied physiology and occupational physiology*, vol. 66, pp. 116–121, 1993. [1](#)
- [8] S. Meunier, J. Kwon, H. Russmann, S. Ravindran, R. Mazzocchio, and L. Cohen, “Spinal use-dependent plasticity of synaptic transmission in humans after a single cycling session,” *The Journal of physiology*, vol. 579, no. 2, pp. 375–388, 2007. [1](#)
- [9] A. K. Thompson and J. R. Wolpaw, “Restoring walking after spinal cord injury: operant conditioning of spinal reflexes can help,” *The Neuroscientist*, vol. 21, no. 2, pp. 203–215, 2015. [1](#)

- [10] A. K. Thompson and J. R. Wolpaw, “H-reflex conditioning during locomotion in people with spinal cord injury,” *The Journal of physiology*, vol. 599, no. 9, pp. 2453–2469, 2021. [1](#)
- [11] K. Kim, T. Akbas, R. Lee, K. Manella, and J. Sulzer, “Self-modulation of rectus femoris reflex excitability in humans,” *Scientific Reports*, vol. 13, no. 1, p. 8134, 2023. [1](#)
- [12] S. J. Harkema, “Neural plasticity after human spinal cord injury: application of locomotor training to the rehabilitation of walking,” *The Neuroscientist*, vol. 7, no. 5, pp. 455–468, 2001. [1](#)
- [13] O. Raineteau and M. E. Schwab, “Plasticity of motor systems after incomplete spinal cord injury,” *Nature Reviews Neuroscience*, vol. 2, no. 4, pp. 263–273, 2001. [1](#)
- [14] M. Hubli and V. Dietz, “The physiological basis of neurorehabilitation-locomotor training after spinal cord injury,” *Journal of neuroengineering and rehabilitation*, vol. 10, no. 1, pp. 1–8, 2013. [1](#)
- [15] H. Lorach, A. Galvez, V. Spagnolo, F. Martel, S. Karakas, N. Interling, M. Vat, O. Faivre, C. Harte, S. Komi, *et al.*, “Walking naturally after spinal cord injury using a brain–spine interface,” *Nature*, pp. 1–8, 2023. [1](#)
- [16] S. Vahdat, O. Lungu, J. Cohen-Adad, V. Marchand-Pauvert, H. Benali, and J. Doyon, “Simultaneous brain–cervical cord fmri reveals intrinsic spinal cord plasticity during motor sequence learning,” *PLoS biology*, vol. 13, no. 6, p. e1002186, 2015. [1](#), [4](#)
- [17] C. Landelle, O. Lungu, S. Vahdat, A. Kavounoudias, V. Marchand-Pauvert, B. De Leener, and J. Doyon, “Investigating the human spinal sensorimotor pathways through functional magnetic resonance imaging,” *NeuroImage*, vol. 245, p. 118684, 2021. [1](#)
- [18] J. D. Brooke and E. P. Zehr, “Limits to fast-conducting somatosensory feedback in movement control,” *Exercise and sport sciences reviews*, vol. 34, no. 1, pp. 22–28, 2006. [1](#)
- [19] J. B. Nielsen and L. G. Cohen, “The olympic brain. does corticospinal plasticity play a role in acquisition of skills required for high-performance sports?,” *The Journal of Physiology*, vol. 586, no. 1, pp. 65–70, 2008. [1](#)
- [20] A. K. Thompson, X. Y. Chen, and J. R. Wolpaw, “Acquisition of a simple motor skill: task-dependent adaptation plus long-term change in the human soleus h-reflex,” *Journal of Neuroscience*, vol. 29, no. 18, pp. 5784–5792, 2009. [1](#)
- [21] A. K. Thompson and J. R. Wolpaw, “The simplest motor skill: mechanisms and applications of reflex operant conditioning,” *Exercise and sport sciences reviews*,



- vol. 42, no. 2, p. 82, 2014. [1](#)
- [22] J. M. Enander, G. E. Loeb, and H. Jörntell, “A model for self-organization of sensorimotor function: spinal interneuronal integration,” *Journal of Neurophysiology*, vol. 127, no. 6, pp. 1478–1495, 2022. [1](#)
- [23] S. O. Verduzco-Flores and E. De Schutter, “Self-configuring feedback loops for sensorimotor control,” *Elife*, vol. 11, p. e77216, 2022. [1](#)
- [24] P. Manoonpong, T. Geng, T. Kulvicius, B. Porr, and F. Wörgötter, “Adaptive, fast walking in a biped robot under neuronal control and learning,” *PLoS Computational Biology*, vol. 3, no. 7, p. e134, 2007. [1](#)
- [25] P. Sar and H. Geyer, “A model for the transfer of control from the brain to the spinal cord through synaptic learning,” *Journal of Computational Neuroscience*, vol. 48, no. 4, pp. 365–375, 2020. [1](#), [2.1](#), [2.2](#), [2.3](#), [2.3.1](#), [4](#), [4.1](#)
- [26] M. Haruno, D. M. Wolpert, and M. Kawato, “Mosaic model for sensorimotor learning and control,” *Neural computation*, vol. 13, no. 10, pp. 2201–2220, 2001. [1](#), [2.3](#), [2.3.1](#), [5](#)
- [27] S. Song and H. Geyer, “A neural circuitry that emphasizes spinal feedback generates diverse behaviours of human locomotion,” *The Journal of physiology*, vol. 593, no. 16, pp. 3493–3511, 2015. [2.1](#)
- [28] N. Hansen and A. Ostermeier, “Adapting arbitrary normal mutation distributions in evolution strategies: The covariance matrix adaptation,” in *Proceedings of IEEE international conference on evolutionary computation*, pp. 312–317, IEEE, 1996. [2.2](#)
- [29] H. Hultborn, “State-dependent modulation of sensory feedback,” *The Journal of physiology*, vol. 533, no. 1, pp. 5–13, 2001. [4](#)
- [30] S. Rossignol, R. Dubuc, and J.-P. Gossard, “Dynamic sensorimotor interactions in locomotion,” *Physiological reviews*, vol. 86, no. 1, pp. 89–154, 2006. [4](#)
- [31] S. Song and H. Geyer, “Evaluation of a neuromechanical walking control model using disturbance experiments,” *Frontiers in computational neuroscience*, vol. 11, p. 15, 2017. [4](#)
- [32] E. Pierrot-Deseilligny and D. Burke, *The Circuitry of the Human Spinal Cord: Its Role in Motor Control and Movement Disorders*. Cambridge University Press, 2005. [4.1](#)